

# Spectrum Similarity-Based Quality Assessment Metric

**Shiva Aghapour Maleki**

Image Processing and Information  
Analysis Lab, Faculty of Electrical and  
Computer Engineering  
Tarbiat Modares University, Tehran,  
Iran  
s\_aghapourmaleki@modares.ac.ir

**Hassan Ghassemian\*** 

Image Processing and Information  
Analysis Lab, Faculty of Electrical and  
Computer Engineering  
Tarbiat Modares University, Tehran,  
Iran  
ghassemi@modares.ac.ir

**Maryam Imani** 

Image Processing and Information  
Analysis Lab, Faculty of Electrical and  
Computer Engineering  
Tarbiat Modares University, Tehran,  
Iran  
maryam.imani@modares.ac.ir

Received: 6 July 2022 – Revised: 21 August 2022 - Accepted: 18 September 2022

**Abstract**—Pansharpening is the fusion of panchromatic (PAN) and multispectral (MS) images to obtain a high spectral and spatial resolution image. Various metrics are introduced to assess the performance of different algorithms of pansharpening. This paper proposes a new metric for spectral quality evaluation of fused images. In the proposed method, spectrum vector of each pixel of fused image is compared to corresponding spectrum of reference image. Area of difference between two spectra is measured, and by applying this process to all pixel vectors of the fused image and taking an average over obtained values, spectral distortion of whole image is obtained. To investigate the efficiency of the proposed index, deliberate spectral distortion is applied to fused image and the proposed metric's ability to detect distortion is examined. Experimental results on real remote sensing images demonstrate the superior performance of the proposed metric compared to other existing metrics.

**Keywords:** Multispectral Image Fusion; Assessment Index; Spectral Distortion; Spectrum; Performance Evaluation.

**Article type:** Research Article



© The Author(s).

Publisher: ICT Research Institute

## I. INTRODUCTION

Several methods have been introduced to fuse panchromatic (PAN) and multispectral (MS) images so far, known as pansharpening [1, 2]. Evaluating the performance of different methods is done by assessing the quality of obtained products. The goal of fusion methods is to provide an image with a high spatial and spectral resolution, while the spectral and spatial distortions are unavoidable during the fusion process. The quality of a fused image is determined by measuring the amount of spectral and spatial distortions [3, 4]. The results of the component substitution (CS) category have a better spatial quality, while the methods of multiresolution analysis (MRA)

category provide pansharpened images with high spectral quality. The attempt of variation optimization (VO) and machine learning (ML) categories is to preserve the spectral and spatial quality of fused images simultaneously [5, 6]. The main issue in assessing the quality of fused images is the unavailability of a reference image. Wald's protocol deals with this challenge by assessing the quality at a reduced resolution [7]; MS and PAN images are down sampled and then fused; the initial MS image is considered as the reference image and the obtained fused image is compared to it. Quality with no reference (QNR) protocol does not require a reference image and assesses the quality at full resolution. It evaluates spectral and spatial distortions of fused

\* Corresponding Author

images by comparing them to initial MS and PAN images, respectively. A combination of two metrics provides the QNR index [8].

The quality of fused images by introduced protocols is assessed using quality assessment metrics. Spectral angle mapper (SAM), erreur relative globale adimensionnelle de synthèse (ERGAS), universe image quality index (UIQI), Q2n, spatial correlation coefficient (SCC) are the most common quality indices [9]. SAM index measures the angle between two spectral vectors. ERGAS calculates the difference between pixels of fused and reference images, the obtained value is normalized by the mean of reference image. UIQI determines the structure similarity of images using three factors including correlation, luminescence and contrast distortions; Q2n is an extension to UIQI. It is designed to evaluate the quality of multiband images, and SCC measures the spatial content of fused images.

Each designed metric evaluates the quality from a different point of view. SAM and ERGAS indices are among the prominent indices in evaluating spectral quality; SCC measures spatial distortion of fused images, and Q2n evaluates the spectral and spatial distortions simultaneously. In this paper, a new index for assessing spectral quality of fused images is proposed based on spectrum similarity. By comparing the spectrum of fused image to reference image, the amount of spectral distortion of pansharpened image could be determined. To assess the proposed index's performance its ability to detect intentional distortion is investigated. Section II describes the proposed index and the method of assessing its performance; section III represents the experimental results, and section IV draws a conclusion.

## II. PROPOSED METHOD

### A. Proposed Index

In this paper, the purpose is to assess the spectral distortion of fused images. An expert observer can

evaluate the quality visually by investigating the color change of fused image called qualitative assessment. Although visual assessment has more reliable results, it is time consuming and expensive. The purpose of this paper is to express visual observations quantitatively. The expert observer compares fused image to reference image and detects any color change or spectral distortion of pixels. The proposed method also seeks to compare the difference between fused and reference images' pixels using a reliable metric. A traditional principle for comparison is to use a functional [10]. A functional ( $F$ ) is called a metric if it has the following properties:

1) Positive definite:

$$F(X, Y) > 0 \quad (1)$$

$$F(X, Y) = 0 \Leftrightarrow X = Y$$

2) Symmetry:

$$F(X, Y) = F(Y, X) \quad (2)$$

3) Triangle inequality:

$$F(X, Z) \leq F(X, Y) + F(Y, Z) \quad (3)$$

Spectrum property is used as desired feature to design a metric to investigate the spectral distortion of fused images.

Spectral distortion is considered as the change of fused image's pixel vector (spectrum) compared to reference image's pixel vector. A higher difference between two spectra indicates a higher distortion. An example of a spectrum comparison of two different pixel vectors of an eight-band fused image to pixel vector of a reference image is shown in Fig. 1. Visual comparison shows more difference (spectral distortion) between pixel vectors of Fig. 1. (a). than pixel vectors of Fig. 1. (b).

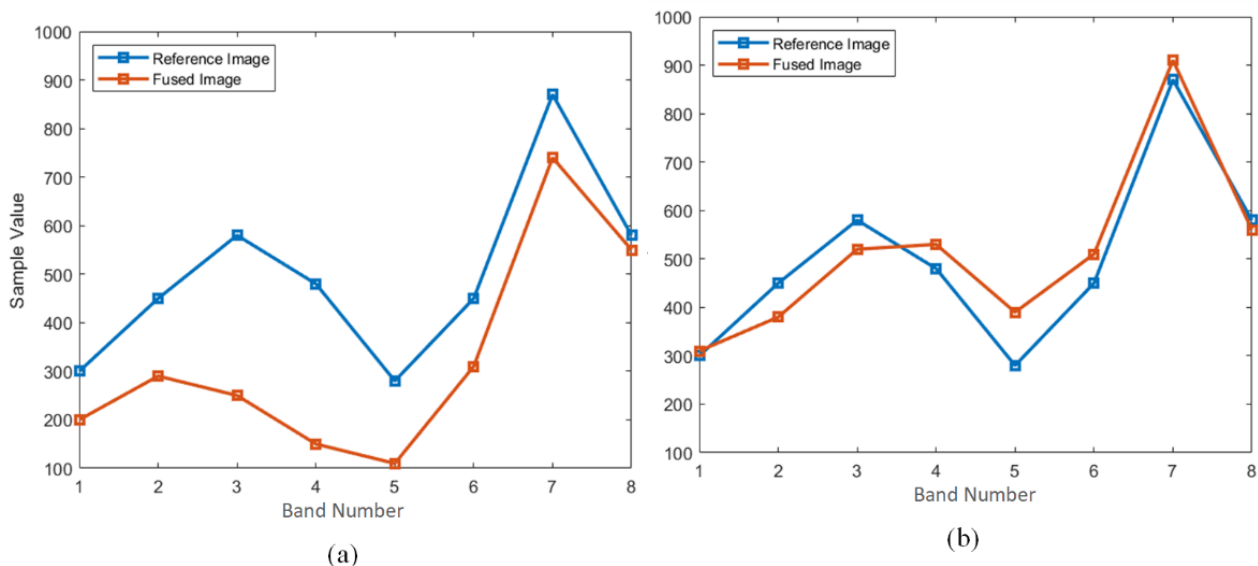


Figure 1. spectrum comparison of fused and reference images (a) high difference between pixel vectors of two images, (b) low difference between pixels vectors of two images.

Since it is impossible to plot the spectrum of all pixels of fused and reference images and compare them visually, difference in spectrum can be quantitatively expressed by calculating the difference area of two spectra:

$$E_i = \int |S_{Fus}^i - S_{Ref}^i| \quad (4)$$

where  $S_{Fus}^i$  and  $S_{Ref}^i$  are the spectra of  $i$ th pixel vector of fused and reference images, respectively and  $E_i$  is the distortion error of  $i$ th pixel vector. Integral operator fulfills triangle inequality [11], area of difference is always non-negative, distortion error would be 0 if two spectra are the same and symmetry property is satisfied because of using absolute value. Therefore, the proposed functional possesses the necessary properties of being a metric and can be used to measure the spectral distortion of corresponding pixels in fused and reference images.

To measure the spectral distortion of whole image, the area of difference of all pixel vectors of fused and reference images is calculated and by taking an average over obtained values, the final spectral distortion value is obtained:

$$E_{image} = \frac{\sum_{i=1}^M E_i}{M \times N} \quad (5)$$

$M$  and  $N$  are the number of image's pixels and bands, respectively and  $E_{image}$  is the total spectral distortion of image.

#### B. Evaluating Performance of the Proposed Index

As mentioned earlier, unavailability of a reference image is a crucial issue in assessing the performance of pansharpening algorithms and quality assessment indices. A solution to this issue could be found in determining the performance of a metric by evaluating its ability in detecting distortion of image [12]. In other words, by applying deliberate distortion in different levels on fused image and assessing the quality of obtained results by desired index, the performance of that index could be determined. It is obvious the measured distortion by index must be increased by increasing distortion level. If an index could not detect the increase in distortion, its reliability is doubtful.

TABLE I. QUANTITATIVE ASSESSMENT OF FUSED IMAGES FOR QUICKBIRD DATA SET.

		SAM	ERGAS	$D_\lambda$	Proposed
	Ideal	0	0	0	0
CS	Brovey	2.188	1.544	0.136	8.299
	GS	1.935	1.456	0.069	7.641
	IHS	2.413	1.705	0.162	8.793
	PCA	1.893	1.318	<b>0.058</b>	6.830
MRA	ATWT	1.795	1.288	0.091	6.504
	AWLP	<b>1.633</b>	<b>1.189</b>	<u>0.063</u>	<b>6.170</b>
	HPF	<u>1.779</u>	<u>1.279</u>	0.086	<u>6.459</u>
	MTF-GLP	1.923	1.673	0.111	8.545

Spectral difference between PAN and MS bands generates spectral distortion. For instance, in CS based pansharpening methods, MS image is transferred to a new space, its spectral and spatial information are separated, and the spatial component is replaced by PAN image; after that, an inverse transform is applied, and the fused image is obtained [13]. If the spatial component has more correlation with the replaced component, the spectral distortion would be less. Therefore, histogram matching is applied to spatial and replaced components before substitution. This way, the replaced component will have the same mean and variance as the spatial component. By changing the mean and variance sameness (histogram mismatching) between PAN and MS images, the fused image will be distorted, and by increasing histogram mismatching percentage, different levels of spectral distortion could be obtained; it is expected from an appropriate and reliable metric to detect these distortions. The performance of proposed and existing prominent spectral metrics will be evaluated using this method in the next section.

### III. EXPERIMENTAL RESULTS

#### A. Assessing Quality of Fused Images

Experiments are performed on two data sets including agricultural and urban areas acquired by QuickBird and GeoEye-1 sensors, respectively. PAN and MS images are of size 1024×1024 and 256×256 pixels. Spatial and spectral resolution of QuickBird sensor is 0.61–0.72 m and 2.44–2.88 m, which MS image has four bands and the spatial and spectral resolution of GeoEye-1 is 0.41 m and 1.65 m, respectively, with four-banded MS image. Fused images are obtained by eight different fusion methods including Brovey [14], Gram-Schmidt (GS) [15], intensity-hue-saturation (IHS) [16], principal component analysis (PCA) [17] from CS category, a trous wavelet transform (ATWT) [18], additive wavelet luminance proportional (AWLP) [19], high-pass filtering (HPF) [20] and modulation transfer function with generalized Laplacian pyramid (MTF-GLP) [21] from MRA category.

TABLE II. QUANTITATIVE ASSESSMENT OF FUSED IMAGES FOR GEOEYE-1 DATA SET.

		SAM	ERGAS	$D_\lambda$	Proposed
	Ideal	0	0	0	0
CS	Brovey	5.437	4.304	<u>0.039</u>	19.438
	GS	<u>5.306</u>	4.227	<b>0.034</b>	19.168
	HIS	5.381	4.258	<u>0.041</u>	19.328
	PCA	5.369	4.240	0.045	19.070
MRA	ATWT	<b>5.202</b>	<b>3.821</b>	0.094	<b>16.816</b>
	AWLP	5.597	<u>4.046</u>	0.074	<u>17.833</u>
	HPF	<u>5.211</u>	<u>3.858</u>	0.091	<u>16.954</u>
	MTF-GLP	5.471	5.150	0.142	22.682



As mentioned earlier, in CS based methods spatial distortion is less than MRA based methods, and MRA based methods preserve spectral information better than CS methods. Therefore, it is expected that MRA based methods have better quantitative results than CS based methods.

Spectral assessment is done using SAM, ERGAS,  $D_\lambda$  (spectral index of QNR protocol) and proposed index. Quantitative assessment results of QuickBird and GeoEye-1 data sets are represented in Table 1 and Table 2 and obtained fused images are illustrated in Fig. 2 and Fig. 3, respectively.

In tables, first rank of each index is shown in bold, second rank with underline and third rank in italics. In QuickBird data set, top three ranks are for ATWT, AWLP and HPF (all from MRA category) methods according to proposed, SAM and ERGAS metrics, while  $D_\lambda$  introduces two methods of CS category as top methods. Top three ranks of this index are from CS category in GeoEye-1 data set. Three methods of MRA category are among top methods according to the proposed and ERGAS metrics. SAM also introduces ATWT and HPF as high-quality methods.

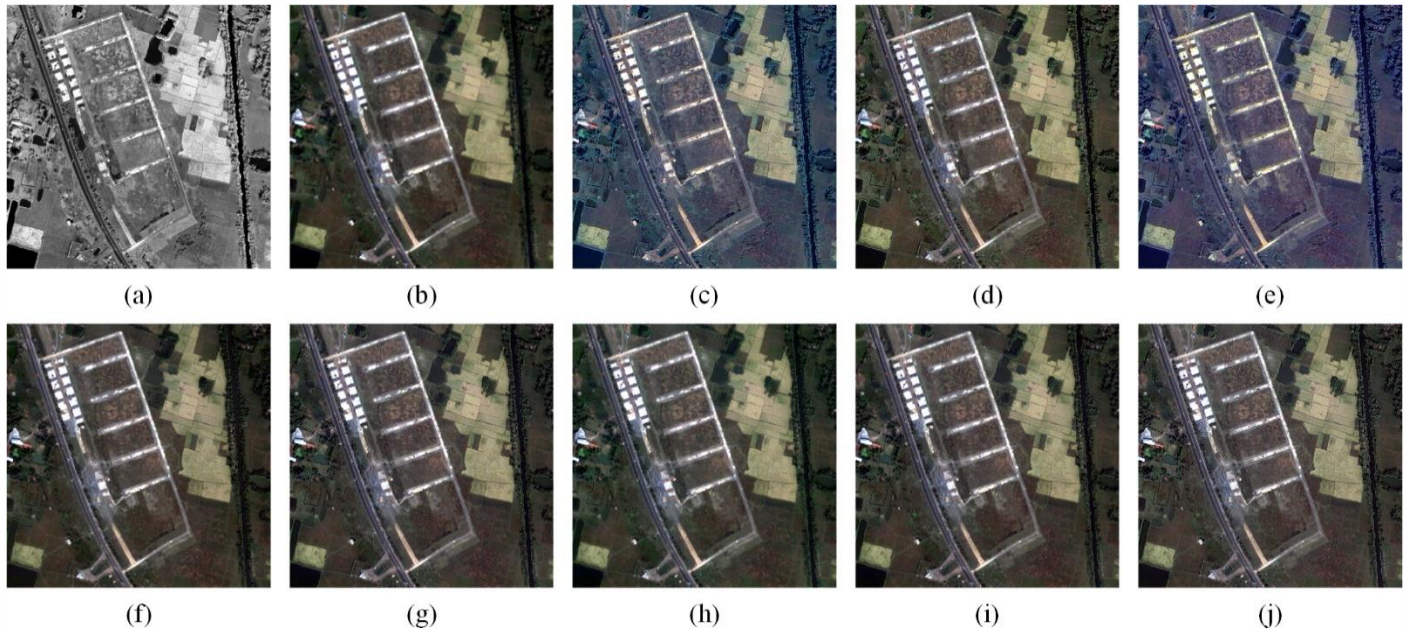


Figure 2. Fusion results of Quickbird data set. (a) PAN, (b) MS, (c) Brovey, (d) GS, (e) IHS, (f) PCA, (g) ATWT, (h) AWLP, (i) HPF, (j) MTF-GLP.

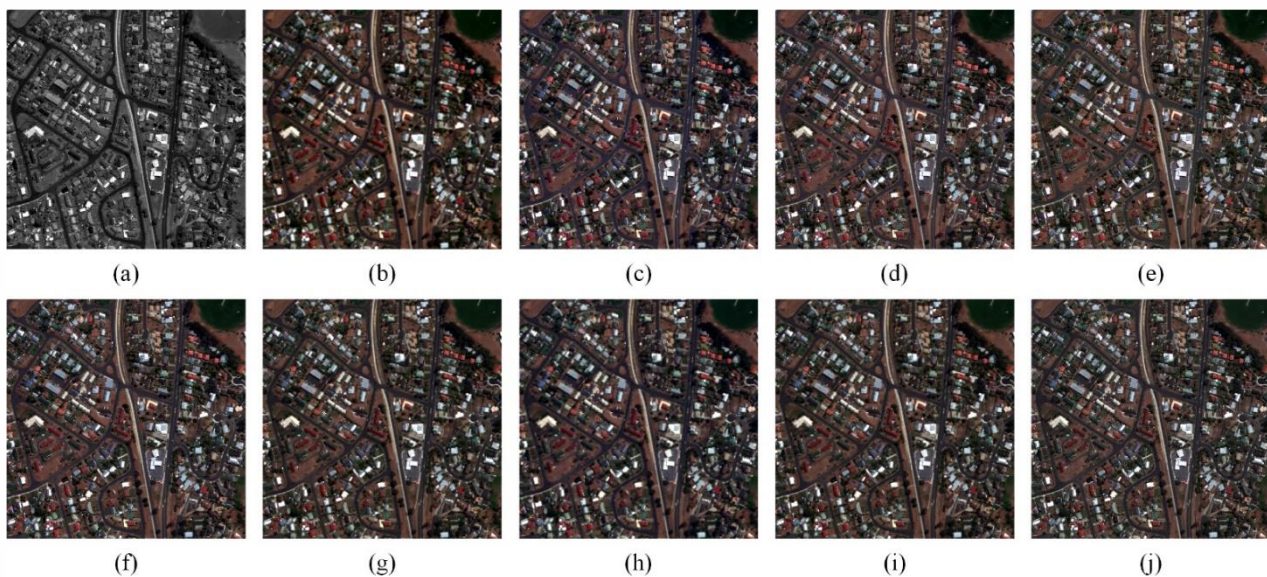


Figure 3. Fusion results of GeoEye-1 data set. (a) PAN, (b) MS, (c) Brovey, (d) GS, (e) IHS, (f) PCA, (g) ATWT, (h) AWLP, (i) HPF, (j) MTF-GLP.



Visual assessment indicates higher spectral distortion of CS methods than MRA methods. Color change of Brovey and IHS methods of QuickBird data set is evident in Fig. 2. By comparing fused images to initial MS image in Fig. 3, it can be seen that spectral distortion of soil and road areas of MRA images is less than CS images. To make a full ranking comparison among quality indices, slope charts of the rankings of metrics are displayed in Fig. 4. According to this figure, the proposed index has the most consistency with ERGAS index in two data sets compared to other two indices. Rankings of proposed and SAM indices are more compatible in QuickBird data set than GeoEye-1 data set. There is a serious contrast between  $D_\lambda$  and proposed index in the rankings of fusion methods. Because of introducing methods from MRA category as high-quality images and relative consistency between proposed and two other indices (SAM and ERGAS), it could be concluded that the proposed index has provided an accurate and acceptable evaluation. In the next section, the performance of proposed, SAM and ERGAS indices in distortion detection is investigated.

#### B. Assessing Performance of Proposed Index

This section discusses the performance of proposed, SAM and ERGAS indices in detecting spectral distortion raised from histogram mismatching between PAN and MS images. In pansharpening methods, mean and variance of PAN and MS images become the same before fusion, known as histogram matching. Instead of the same mean and variance, amounts of 5%, 10%, 15% and 20% difference between mean and variance of MS and PAN images are applied to provide histogram mismatching and

desired spectral distortion levels. The proposed and existing quality metrics are expected to detect different levels of distortions. Therefore, mismatched PAN and MS images are fused using different fusion methods and assessed by SAM, ERGAS and proposed metrics; to compare the performance of indices in detecting the occurred distortions, obtained values by each metric are normalized. In the normalization step, the result of distortion free image (fused image obtained by histogram matching) is considered as reference and the quality results of distorted images are divided by this value. In this way, comparing the increment rate of assessment results by increasing distortion levels allows performance investigation of metrics. Comparative graphs of metrics' assessment results for QuickBird and GeoEye-1 data sets are depicted in Fig. 5 and Fig. 6, respectively. In these figures, the horizontal axis indicates the percentage of applied histogram mismatching to PAN and MS images and the vertical axis represents the normalized distortion value. PAN and MS images are fused using four pansharpening methods. The increment rate of the proposed index is higher than other two indices for Brovey and IHS fusion methods. SAM index has the poorest performance; this index could not make a distinction among distortion levels of Brovey method and reports the same results for distorted free and all levels of distorted images in both data sets. ERGAS index indicates an increase in the quality of 5% distorted image compared to the distortion free image for Brovey and IHS methods in GeoEye-1 data set. Also, the quality of 10% distorted image is as same as the quality of distortion free image for Brovey method in this data set according to this index.

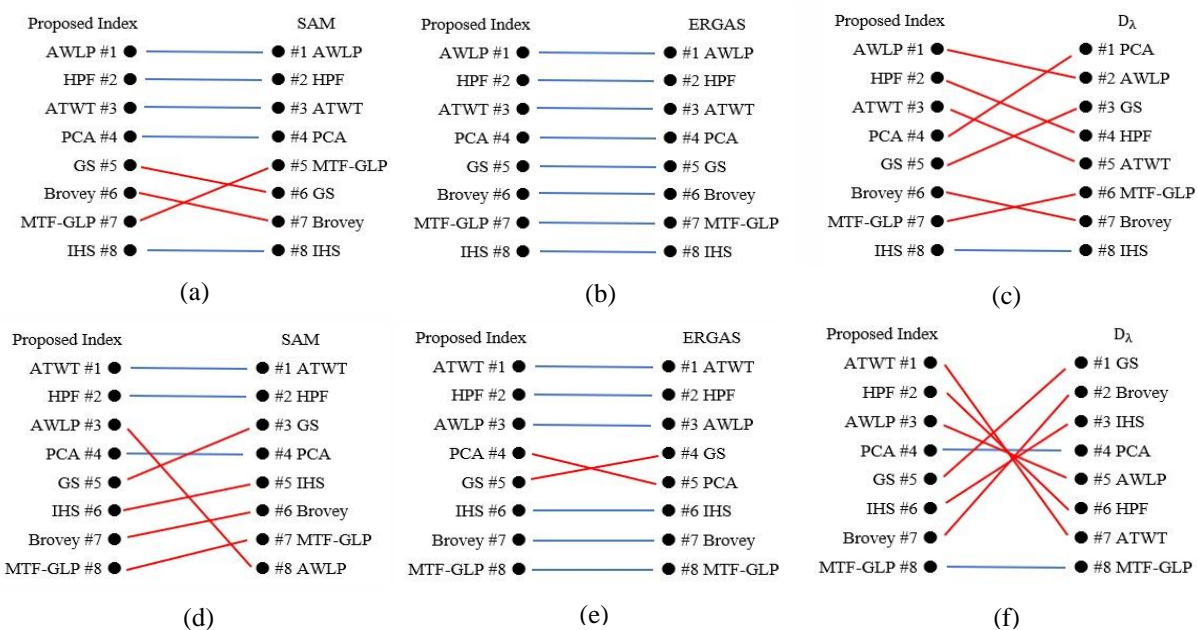
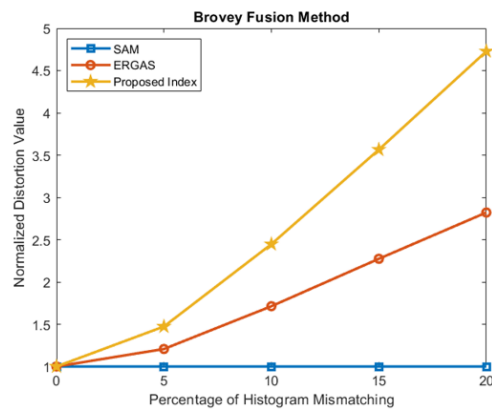
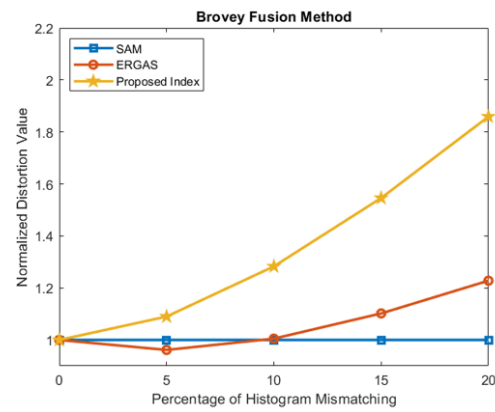


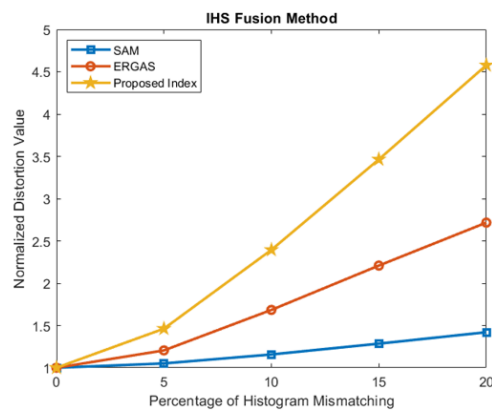
Figure 4. Slope Charts of the proposed and (a), (d) SAM, (b), (e) ERGAS, (c), (f)  $D_\lambda$  rankings for QuickBird and GeoEye-1 data sets.



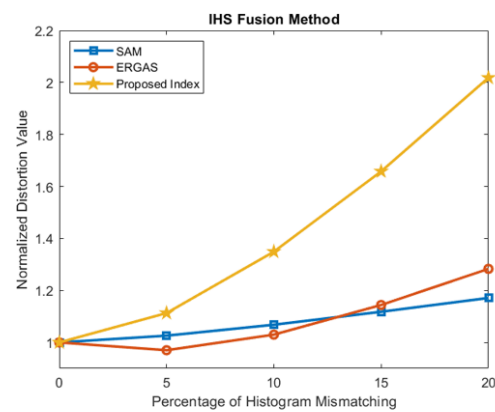
(a)



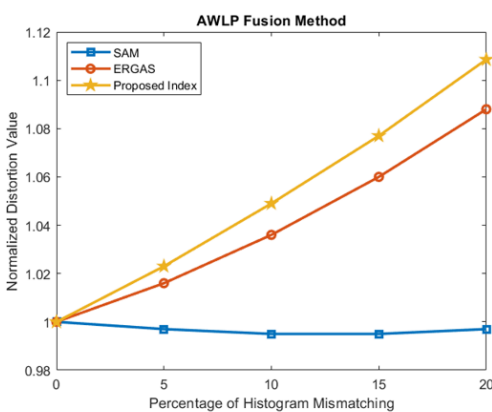
(a)



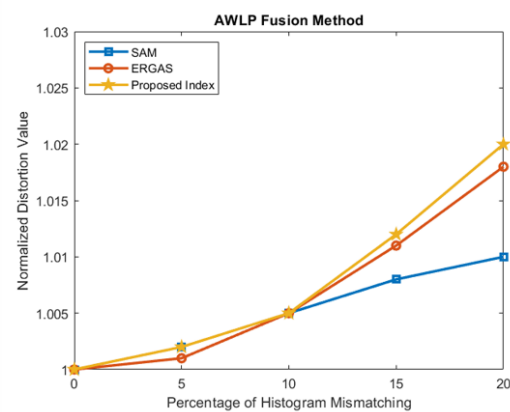
(b)



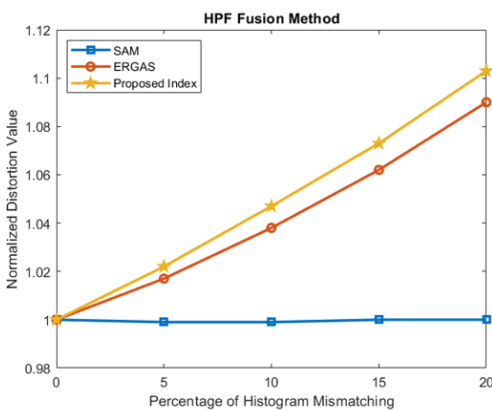
(b)



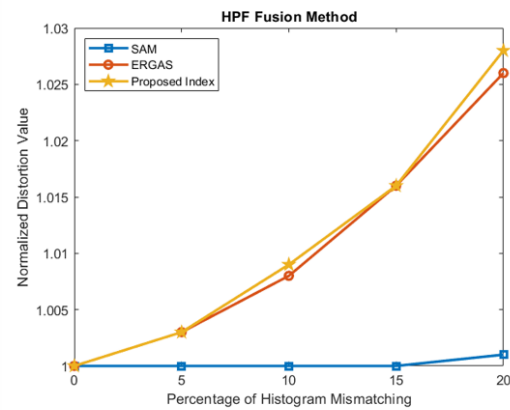
(c)



(c)



(d)



(d)

Figure 5. Comparative charts of metrics on QuickBird data set. (a) Brovey, (b) IHS, (c) AWLP, (d) HPF.

Figure 6. Comparative charts of metrics on GeoEye-1 data set. (a) Brovey, (b) IHS, (c) AWLP, (d) HPF.



According to three metrics, AWLP and HPF methods do not significantly differ in quality results for different levels of distortion. However, proposed index represents the slight difference among distortion levels better than other metrics. For visual comparison, distortion free and distorted fused images obtained by Brovey and AWLP methods are shown in Fig. 7. Spectral distortion of Brovey image is increased by increasing the histogram mismatching percentages. Also, as can be seen in this figure, color change of QuickBird data set is more than GeoEye-1. The reason is that vegetation diversity makes agricultural areas

more sensitive to pixel change and spectral distortion, so spectral assessment of such areas is more important than urban areas, and a practical index is expected to sense even the slight change of pixels. The proposed index has acted successfully in this field because, as seen in Fig. 5 and Fig. 6, slope increment of measured distortions of QuickBird data set is more than GeoEye-1. According to slope charts and visual observation, histogram mismatching does not significantly impact spectral quality of images obtained by methods of MRA category, which indicates the robustness of MRA methods to histogram mismatching.

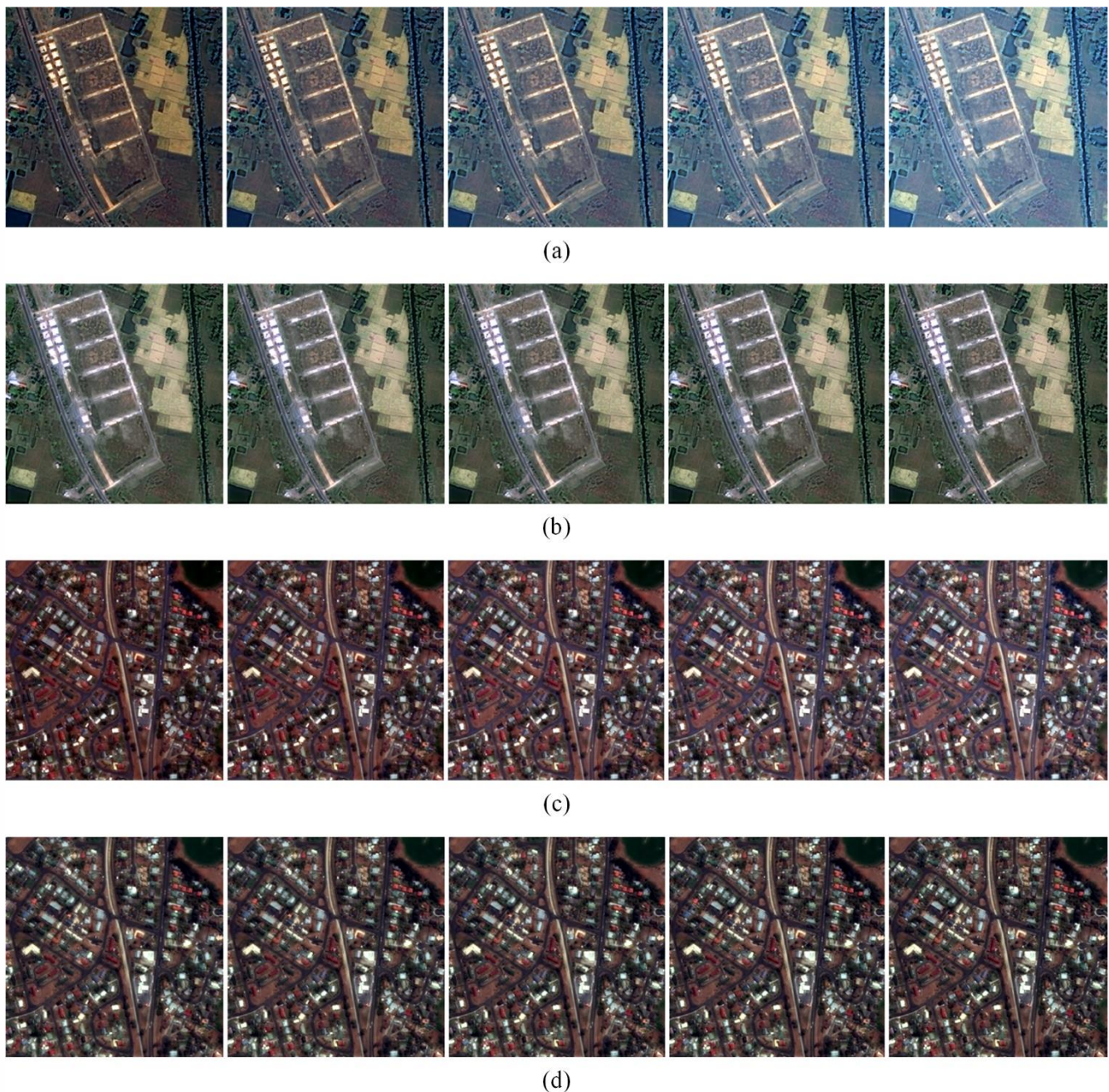


Figure 7. Distortion free and distorted fused images obtained by 5, 10, 15, and 20 percentages of histogram mismatching (left to right), fused by (a), (c) Brovey, (b), (d) AWLP on QuickBird and GeoEye-1 data sets.



## IV. CONCLUSION

In this paper, a new spectral quality assessment metric is proposed. The metric measures the spectral distortion of fused images based on spectrum similarity. In the Experimental Results section, the quality of fused images was evaluated using the proposed index. Since there is no reference image to evaluate the performance of introduced metrics for pansharpened image quality assessment, deliberate spectral distortion in different levels was applied to fused images to investigate the performance of existing and proposed metrics in finding distortions. Different percentages of histogram mismatching were applied to MS and PAN images before fusion process to produce desired distortion. By assessing obtained fused images using SAM, ERGAS and proposed metrics, the proposed index showed the quality distinction of different distortion levels better than other metrics for Brovey and IHS methods. Also, numerical results and visual observation represented the robustness of methods of MRA category to histogram mismatching.

Since spatial quality evaluation is also a critical subject in quality evaluation of fused images, by introducing a reliable spatial index and combining it with the proposed spectral index, a total index can be reached for simultaneous spectral and spatial quality evaluation of fused images.

## REFERENCES

- [1] H. Ghassemian, "A review of remote sensing image fusion methods," *Information Fusion*, vol. 32, pp. 75-89, 2016.
- [2] L. Alparone, L. Wald, J. Chanussot, C. Thomas, P. Gamba, and L. M. Bruce, "Comparison of pansharpening algorithms: Outcome of the 2006 GRS-S data-fusion contest," *IEEE Transactions on Geoscience and Remote Sensing*, vol. 45, no. 10, pp. 3012-3021, 2007.
- [3] S. Aghapour Maleki and H. Ghassemian, "A pansharpened image quality assessment using segmentation procedure," *International Journal of Remote Sensing*, vol. 42, no. 11, pp. 4157-4176, 2021.
- [4] G. Scarpa and M. Ciotola, "Full-resolution quality assessment for pansharpening," *Remote Sensing*, vol. 14, no. 8, p. 1808, 2022.
- [5] G. Vivone et al., "A new benchmark based on recent advances in multispectral pansharpening: Revisiting pansharpening with classical and emerging pansharpening methods," *IEEE Geoscience and Remote Sensing Magazine*, vol. 9, no. 1, pp. 53-81, 2020.
- [6] Z.-R. Jin, Y.-W. Zhuo, T.-J. Zhang, X.-X. Jin, S. Jing, and L.-J. Deng, "Remote Sensing Pansharpening by Full-Depth Feature Fusion," *Remote Sensing*, vol. 14, no. 3, p. 466, 2022.
- [7] L. Wald, T. Ranchin, and M. Mangolini, "Fusion of satellite images of different spatial resolutions: Assessing the quality of resulting images," *Photogrammetric engineering and remote sensing*, vol. 63, no. 6, pp. 691-699, 1997.
- [8] L. Alparone, B. Aiazzi, S. Baronti, A. Garzelli, F. Nencini, and M. Selva, "Multispectral and panchromatic data fusion assessment without reference," *Photogrammetric Engineering & Remote Sensing*, vol. 74, no. 2, pp. 193-200, 2008.
- [9] G. Vivone, M. Dalla Mura, A. Garzelli, and F. Pacifici, "A benchmarking protocol for pansharpening: Dataset, preprocessing, and quality assessment," *IEEE Journal of Selected Topics in Applied Earth Observations and Remote Sensing*, vol. 14, pp. 6102-6118, 2021.
- [10] H. Ghassemian and D. Landgrebe, "Multispectral image compression by an on-board scene segmentation," in *IGARSS 2001. Scanning the Present and Resolving the Future. Proceedings. IEEE 2001 International Geoscience and Remote Sensing Symposium* (Cat. No. 01CH37217), 2001, vol. 1: IEEE, pp. 91-93.
- [11] R. L. Schilling, *Measures, integrals and martingales*. Cambridge University Press, 2017.
- [12] F. D. Javan, F. Samadzadegan, S. Mehravar, and A. Toosi, "A review on spatial quality assessment methods for evaluation of pan-sharpened satellite imagery," *The International Archives of Photogrammetry, Remote Sensing and Spatial Information Sciences*, vol. 42, pp. 255-261, 2019.
- [13] G. Vivone et al., "A critical comparison among pansharpening algorithms," *IEEE Transactions on Geoscience and Remote Sensing*, vol. 53, no. 5, pp. 2565-2586, 2014.
- [14] A. R. Gillespie, A. B. Kahle, and R. E. Walker, "Color enhancement of highly correlated images. II. Channel ratio and "chromaticity" transformation techniques," *Remote Sensing of Environment*, vol. 22, no. 3, pp. 343-365, 1987.
- [15] C. A. Laben and B. V. Brower, "Process for enhancing the spatial resolution of multispectral imagery using pansharpening," ed: Google Patents, 2000.
- [16] W. Carper, T. Lillesand, and R. Kiefer, "The use of intensity-hue-saturation transformations for merging SPOT panchromatic and multispectral image data," *Photogrammetric Engineering and remote sensing*, vol. 56, no. 4, pp. 459-467, 1990.
- [17] P. Kwarteng and A. Chavez, "Extracting spectral contrast in Landsat Thematic Mapper image data using selective principal component analysis," *Photogramm. Eng. Remote Sens.*, vol. 55, no. 1, pp. 339-348, 1989.
- [18] M. J. Shensa, "The discrete wavelet transform: wedding the a trous and Mallat algorithms," *IEEE Transactions on signal processing*, vol. 40, no. 10, pp. 2464-2482, 1992.
- [19] X. Otazu, M. González-Audicana, O. Fors, and J. Núñez, "Introduction of sensor spectral response into image fusion methods. Application to wavelet-based methods," *IEEE Transactions on Geoscience and Remote Sensing*, vol. 43, no. 10, pp. 2376-2385, 2005.
- [20] T.-M. Tu, S.-C. Su, H.-C. Shyu, and P. S. Huang, "A new look at IHS-like image fusion methods," *Information fusion*, vol. 2, no. 3, pp. 177-186, 2001.
- [21] L. Alparone, A. Garzelli, and G. Vivone, "Intersensor statistical matching for pansharpening: Theoretical issues and practical solutions," *IEEE Transactions on Geoscience and Remote Sensing*, vol. 55, no. 8, pp. 4682-4695, 2017.



**Shiva Aghapour Maleki** received the B.Sc. and M.Sc. degrees in Electrical Engineering from University of Tabriz, Tabriz, Iran in 2014 and 2017 respectively and the Ph.D. degree in Electrical Engineering from Tarbiat Modares University, Tehran, Iran in 2022. Her research interests include Signal Processing, Image Processing, Remote Sensing and Machine Learning.



**Hassan Ghassemian** received the B.Sc. degree in Electrical Engineering from Tehran College of Telecommunication in 1980 and the M.Sc. and Ph.D. degrees in Electrical Engineering from Purdue University, West Lafayette, USA in 1984 and 1988 respectively. Since 1988, he has been with Tarbiat Modares University in Tehran, Iran, where he is a Professor of Computer and Electrical Engineering. His research interests focus on Multi-Source Signal/Image Processing and Information Analysis and Remote Sensing.





**Maryam Imani** completed her Ph.D in Electrical Engineering, from Tarbiat Modares University, Tehran, Iran in 2015. She continued her research in Tarbiat Modares University as a postdoc. Since 2018, she has been with Tarbiat Modares University in Tehran, Iran, where she is the Associate Professor of Computer and Electrical Engineering. Her research interests include Remote Sensing, Statistical Pattern Recognition, Signal and Image Processing, and Machine Learning.